JOURNAL OF SPACECRAFT AND ROCKETS
Vol. 36, No. 1, January–February 1999

Probability of Structural Failure of a Satellite Launching Motor: Case Study

Giora Maymon*
RAFAEL, Ministry of Defense, 31021 Haifa, Israel

A solution-treated and aged titanium alloy pressure vessel that was developed for the upper-stage rocket motor used in the Israeli space program failed during a pressure test. Investigation of the production data revealed the existence of geometrical imperfections (out-of-roundness), which were less than 0.5% of the nominal radius of the pressure vessel. Finite element deterministic analysis was used to formulate a closed-form failure function, based on Taylor series expansion of the deterministic solutions. Indeterministic rupture strains and residual stresses were assumed, and the probabilities of failure were calculated for different values of imperfections. Structural probabilistic analysis demonstrated the dramatic effect that such small imperfections may have on a nominal design.

Nomenclature

G	= failure function
L	= reference length, 50 mm
p	= internal pressure, atm
p_e	= pressure around which Taylor expansion is evaluated, atm
R	= radius of the motor case, mm
$\{S\}$	= matrix of deterministic solutions for stresses, kg/mm^2
S_i	= residual stress, kg/mm^2
s	= running coordinate along the shell, mm
t	= shell thickness, 1.7 mm
$[Y]$	= matrix of differences
α_i	= Taylor series coefficients, where i is 0, 1, 2, 3
ΔR	= change in motor case radius, mm
δ	= double amplitude of out-of-roundness, mm
ε	= strain
σ_R	= rupture stress, kg/mm^2
$\sigma_{Y \mid \delta = \text{const}}$	= stress in the Y direction for a constant δ, kg/mm^2

Introduction

THE AUS-51 (Fig. 1) is a solid-propellant upper-stage rocket motor that is used in the Israeli space program. The motor case, a spherical shell of 1300-mm diam, has a total weight of 2007 kg, of which 94.2% is the propellant. The spherical motor case, which was used during the project development and the first two satellite launchings, was made of annealed (AN) Ti-6Al-4V titanium alloy. It was fabricated out of 12 segments of machined titanium plates shaped by press forming and welded together by an electron beam process.

A change in the case material to a solution-treatedand aged (STA) titanium alloy was suggested. The reason for this possible modification was an expected reduction of structural weight by approximately 10%, resulting in a 1:1 gain in the possible payload weight of the satellite. The modified version has the same general configuration of the original design, except for a reduction in the spherical shell thickness.

A prototype of the modified motor case (STA0) was developed, fabricated, and successfully tested. Three additional specimens (motor cases STA1, 2, and 3) were then fabricated, the first for additional structural testing, the second for ground firing, and the third for the next satellite launching. Each case was successfully proof tested after production.

In a pressure test of STA1, the motor case, which is essentially a pressure vessel, burst at a pressure that was 80% of the design minimum-burst pressure. In the investigation that followed the test failure, it was found that, whereas the AN cases had an out-of-roundness double amplitude of 0.5 mm and the first prototype (STA0) of 0.75 mm, the STA1, 2, and 3 specimens exhibited values of 3-mm double amplitude over the nominal radius of 650 mm. This out-of-roundness caused very high local stresses during the pressure test. The origin of these larger imperfections obtained in the production is still unknown.

To demonstrate the possibility of failure due to these imperfections, deterministic and probabilistic analyses were carried out. The deterministic analysis was based on finite element analysis using the ANSYS[1] program, and as a result, a closed-form function for the maximum stress (stress response surface) was generated. The probabilistic analysis was performed using the PROBAN[2] program, and rupture and residual stresses were considered indeterministic. Pressure and out-of-roundness amplitude were changed parametrically; thus, they were considered deterministic for each computation.

Deterministic Finite Elements Analysis

A large-deflections elastoplastic finite element analysis was used for calculating the maximum stresses in the critical location of the pressure vessel, the regions where thickness is step changed by the machining process. The production imperfections were measured along the equator of the spherical pressure vessel, and due to the symmetry, only a sector of 15 deg (half a sector) of this cross section, subjected to internal pressure loading, was analyzed. In this sector, shown in Fig. 2, the initial imperfection (out-of-roundness) was assumed to be

$$\Delta R(s) = -(\delta/2)[1 + \cos(\pi s/L)] \tag{1}$$

where δ was assumed to take the values of 0, 1.3, 2, and 3 mm and L was fixed at 50 mm. This value was selected arbitrarily due to the fast decay of local bending stresses as a function of the running distance s. This form of imperfection function is a good representation for the calculations of the stresses (in the Y direction) at the location of thickness changes. The appropriate boundary conditions (symmetry) are also shown in Fig. 2. The STA titanium alloy stress-strain curve[3] was approximated by the two slopes model shown in Fig. 3.

In Fig. 4 the maximum stress in the Y direction is shown as a function of the internal pressure for four values of the initial imperfection double amplitude. A close-up on the results for the internal pressure range of interest is also shown in Fig. 4.

Received Jan. 12, 1998; revision received June 24, 1998; accepted for publication July 24, 1998.

*Research Fellow, Aerodynamic Systems Department, Missiles Division, P.O. Box 2250, MS 39. E-mail: gioram@netvision.net.il. Associate Fellow AIAA.

Fig. 1 AUS-51 upper-stage motor.

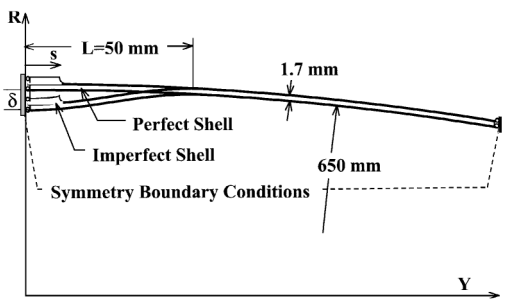

Fig. 2 Section geometry for the finite element analysis.

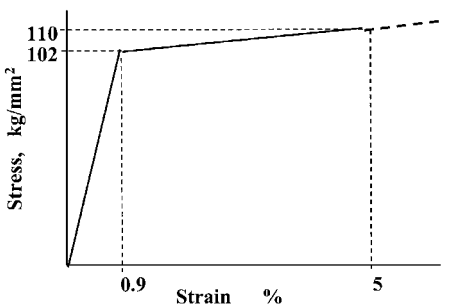

Fig. 3 Stress–strain curve for STA alloy (approximated).

Deterministic Closed-Form Expression (Stress Response Surface)

The nature of the curves in Fig. 4 suggests that (at least) a cubic closed-form expression is required for the relationship between the maximum stress and the acting pressure (the stress response surface). Thus, the following function was assumed:

$$\sigma_y|_{\delta=\text{const}} = \alpha_0 + \alpha_1(p - p_e) + \alpha_2(p - p_e)^2 + \alpha_3(p - p_e)^3 \quad (2)$$

where p_e is the point around which a Taylor series expansion is made and α_i ($i = 0, 1, 2, 3$) are unknown coefficients. The midrange value of $p_e = 44$ atm was selected, and the expansion was made for pressure values of 36, 38, 40, 42, 46, 48, 50, and 52 atm. The matrix

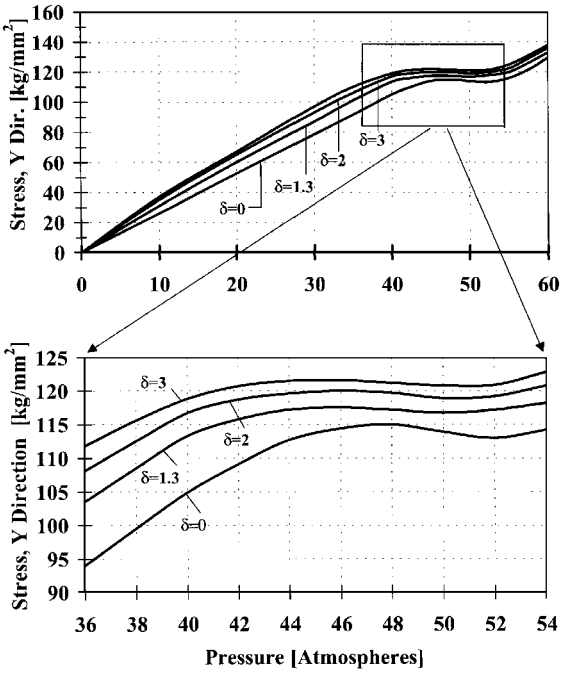

Fig. 4 Maximum stress in the Y direction.

$[Y]$ of the differences between the evaluation point and the other pressure values is

$$[Y] = \begin{bmatrix} 1 & -8 & 64 & -512 \\ 1 & -6 & 36 & -216 \\ 1 & -4 & 16 & -64 \\ 1 & -2 & 4 & -8 \\ 1 & 0 & 0 & 0 \\ 1 & 2 & 4 & 8 \\ 1 & 4 & 16 & 64 \\ 1 & 6 & 36 & 216 \\ 1 & 8 & 64 & 512 \end{bmatrix} \quad (3)$$

Four sets of ANSYS deterministic solutions for nine pressure values were calculated:

$$\{S\}|_{\delta=0} = \begin{Bmatrix} 94.0 \\ 99.5 \\ 104.9 \\ 109.1 \\ 112.7 \\ 114.4 \\ 115.0 \\ 113.9 \\ 113.0 \end{Bmatrix}, \quad \{S\}|_{\delta=1.3} = \begin{Bmatrix} 103.5 \\ 108.5 \\ 113.3 \\ 115.8 \\ 117.2 \\ 117.5 \\ 117.2 \\ 116.7 \\ 117.2 \end{Bmatrix}$$

$$\{S\}|_{\delta=2} = \begin{Bmatrix} 108.1 \\ 112.5 \\ 116.7 \\ 118.7 \\ 119.6 \\ 120.0 \\ 119.7 \\ 118.9 \\ 119.2 \end{Bmatrix}, \quad \{S\}|_{\delta=3} = \begin{Bmatrix} 111.8 \\ 115.6 \\ 118.8 \\ 120.7 \\ 121.5 \\ 121.6 \\ 121.2 \\ 120.8 \\ 120.9 \end{Bmatrix} \quad (4)$$

Table 1 Coefficients for Taylor series

Coefficient	$\delta = 0$	$\delta = 1.3$	$\delta = 2$	$\delta = 3$
α_0	112.2727	116.9723	119.6195	121.3662
α_1	1.274369	0.401136	0.293350	0.224074
α_2	−0.14148	−0.10711	−0.09656	−0.08082
α_3	−0.00145	0.007197	0.006303	0.005440

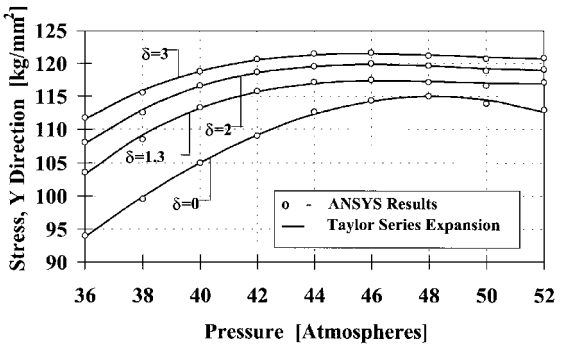

Fig. 5 Comparison of the ANSYS solutions and closed-form Taylor series expansion.

The best set of coefficients α_i $(i = 0, 1, 2, 3)$ can be obtained by solving[4]

$$[Y]^T[Y]\{\alpha\} = [Y]^T\{S\} \tag{5}$$

In Table 1, the coefficients for Eq. (2) obtained by solving Eq. (5) with the data of Eqs. (3) and (4) are summarized.

In Fig. 5 the ANSYS results [Fig. 4 and Eqs. (4)] and the Taylor series approximations are shown. A very good curve fitting is obtained; thus, Eq. (2) with the coefficients of Table 1 can be used as a closed-form expression (a stress response surface) for the maximum stress values.

Failure Criterion

The determination of a failure criterion for a structural system depends on the design specifications and on an understanding of the structural behavior. In many traditional designs the failure is defined by the beginning of plastic deformations in the structure. This is a conservative approach that does not take into account some plastic deformation that may be allowed in a structure, especially in the one discussed in this paper. Plastic deformation may result in the generation of a very small crack and a redistribution of the stresses in such a way that the total structure is still safe. In such a case, a thorough analysis must be performed when the structure is subjected to more than one loading step, due to the possibility of the propagation of such a crack. A rigorous analysis may require the application of a heavy three-dimensional numerical analysis.

For the purpose of the present simplified analysis, a very simple failure criterion was adopted. It was assumed that the pressure vessel fails when the stress in a certain point reaches the rupture stress. Rupture stress is determined as a result of the value of the rupture strain. The latter is assumed to take different parametric values in the deterministic analysis and to be a random variable in the probabilistic analysis. The relationship between the rupture stress and strain is assumed to follow the plastic zone of the stress–strain curve presented in Fig. 3. Thus, the rupture stresses that correspond to given values of rupture strains are those described in Table 2.

Deterministic Failure Analysis

Using the defined failure criterion, the calculated coefficients (Table 1) and the calculated stresses [Eq. (2)], it is possible to calculate deterministically the pressure in which the structure fails. To include in the parametric analysis the possibility of an internal residual stress S_i in the Y direction (which may exist in the structure after the postwelding thermal treatment of the structure), the following equation is written:

$$\sigma_Y = \sigma_{y\,|\,\delta = \text{const}} + S_i \tag{6}$$

Table 2 Rupture stresses and strains

Strain, %	Stress, kg/mm²
4	108
5	110
6	112
7	114
8	116
9	118

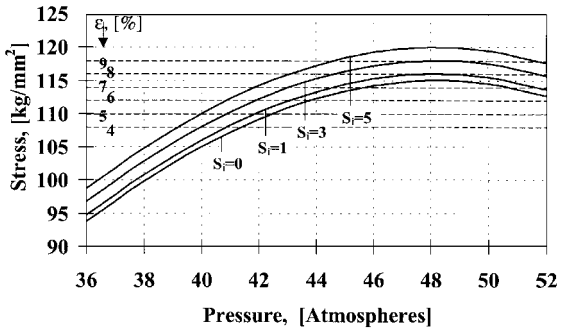

Fig. 6 Calculated stresses and strains, $\delta = 0$.

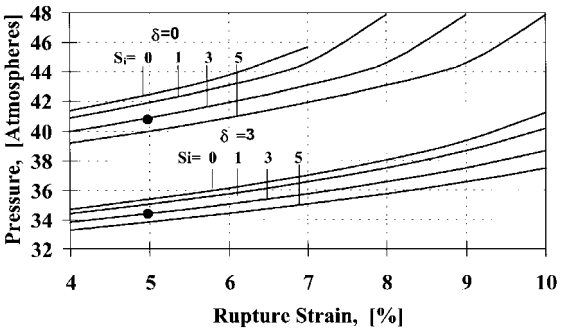

Fig. 7 Deterministic failure map.

where the first term is calculated by Eq. (2) and the second term is a parameter. Equation (6) is shown in Fig. 6 for the case $\delta = 0$ and for four residual stresses. Note the ε scale on the vertical axis, which is plotted using the data of Table 2. Similar curves were drawn for other values of δ but are not shown here.

In Fig. 7 a map of failure points is shown for $\delta = 0$ and for $\delta =$ 3 mm. For example, when the rupture strain is 5%, the residual stress 3 kg/mm^2, and the imperfection amplitude 3 mm, the failure pressure is 34.5 atm. For the same rupture strain and residual stress, the failure pressure of a perfect shell ($\delta = 0$) is 41 atm. Thus, a reduction of 16% in failure pressure is obtained due to a 3-mm imperfection. It can also be seen that the effect of the assumed residual stress on the failure pressure is much smaller than the effect of the imperfection double amplitude.

Variables for Nondeterministic Analysis

To perform a probabilistic structural analysis, the different variables of the problem, p, δ, t, S_i, and σ_R, should be defined.

1) The behavior of the structure loaded by a given pressure p is examined. Therefore, p was assumed to be a deterministic variable, used as a parameter in the computations.

2) Because of the small number of specimens in this case study, there are not enough data to define a probability density function for the imperfection amplitude δ obtained in the production process. Therefore, these imperfections are considered as deterministic parameters. The analysis can be easily expanded to include δ as a random variable once enough data are collected.

3) All of the finite element analyses were performed for a deterministic nominal motor case thickness $t = 1.7$ mm.

4) The residual stresses S_i are very difficult to measure, and their probability distributions even more difficult to define. Therefore,

their effect was analyzed parametrically for four deterministic values and for three probability density functions: a) uniform distribution between 0 and 5 kg/mm^2; b) normal distribution, with zero mean and 1.667 kg/mm^2 standard deviation, which allows negative residual stresses; and c) one-sided normal distribution with lowest value equal to zero and a standard deviation of 1.667 kg/mm^2.

5) The rupture stress σ_R of STA titanium was assumed to behave according to a Hermite transformation model described in Refs. 5 and 6. The selected statistical moments were 114 kg/mm^2 for the mean (average strain of 7%), 1.5 kg/mm^2 for the standard deviation, −1.5 for the skewness, and 1.5 for the kurtosis. This distribution gives more weight to the 7–8% rupture strain range, and in 90% of the cases, the rupture strains are higher than 6%. Such a distribution is supported by limited data supplied by the metallurgists.

Probabilistic Failure Analysis

The formulation of the structural probabilistic problem is, "What is the probability of failure of the motor case under a given internal pressure p, when the structure has an imperfection amplitude δ, a random residual stress S_i, and a random rupture stress σ_R?"

The basic concepts of probabilistic analysis of structures are not repeated in this paper. Methods for application of these concepts

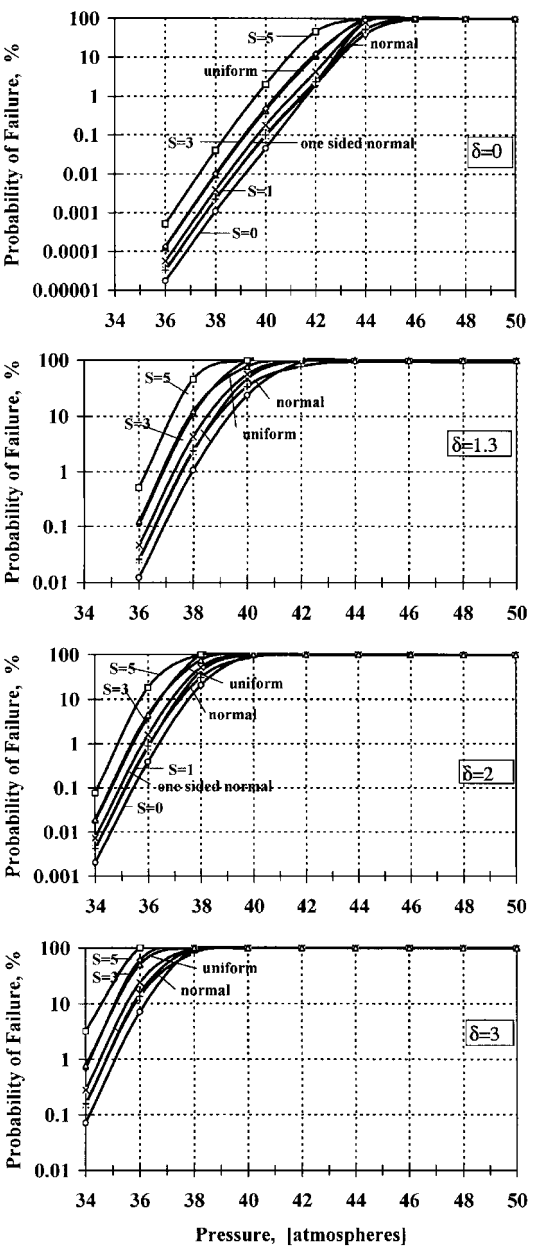

Fig. 8 Probability of failure, four values of δ.

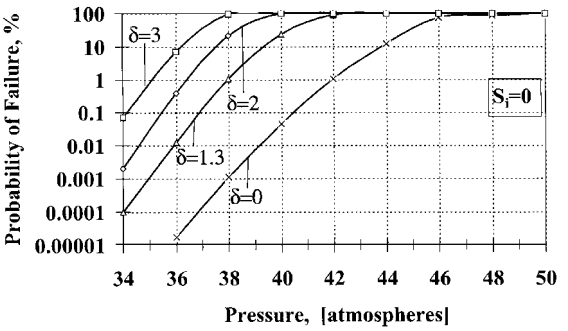

Fig. 9 Probability of failure, no residual stresses.

to engineering problems are described in Ref. 7. It is a standard procedure to solve such problems by creating a failure function, which describes a multidimensional surface that separates the fail and the safe regions. Then, the probability of the system being in the fail region is calculated.

Using the failure criterion described earlier, a failure function G can be written as

$$G = \sigma_R - (\sigma_{y\,|\,\delta=\text{const}} + S_i) \tag{7}$$

Structural failure occurs when $G \leq 0$. The probability of failure was calculated using the PROBAN[2] program. Second-order reliability methods[7] were used.

Results for $\delta = 0$, 1.3, 2, and 3 mm are shown in Fig. 8 for the perfect motor case. Each part in Fig. 8 includes four deterministic residual stresses (0, 1, 3, and 5 kg/mm^2), three random residual stress distributions (uniform, normal, and one-sided normal), and Hermite transformation model probability distribution of the rupture stresses.

The probability of failure for zero residual stresses and for four initial imperfection values is shown in Fig. 9. Similar curves were obtained for other values of S_i. A dramatic influence of δ on the probability of failure of the motor case can be seen from the results presented in Fig. 9.

Discussion

Deterministic solutions such as those described in Fig. 7 can predict the influence of some structural parameters, i.e., residual stresses and initial imperfections, on the failure pressure of the described pressure vessel. Nevertheless, the effect is much more dramatically demonstrated using the probabilistic approach. For example, for a perfect motor case, $\delta = 0$, with no residual stresses, $S = 0$, the probability of failure at an internal pressure of 36 atm is 0.000015% (Fig. 9). When an imperfection amplitude of 3 mm (less than 0.5% of the radius) is introduced, this probability is increased to a value of 10%, which is clearly unacceptable for a practical design. This large increase was obtained using very engineering-reasonable assumptions on the possible dispersion of the rupture stress.

Conclusion

The case study presented can serve four major purposes.

1) It explains, by statistical argumentation, the possible reason for the failure of the tested motor case.

2) It demonstrates the large influence of the initial out-of-roundness of the shell on the probability of failure of the structure (and, therefore, its survivability). This may influence production control methods.

3) It can direct the designers and the production engineers as to what kind of statistical data should be collected in the production process so that better designs can be performed in the future.

4) It demonstrates the advantages of performing a probabilistic structural analysis. Although a very simple model was used, it shows the effects of various parameters on the survivability of the structure. More advanced failure criteria can be used, other probability density functions can be tested, and additional parameters can be randomized.

It is believed that probabilistic failure analysis is a key technology in the future analysis procedures of high-performance systems, and the use of such analysis can result in better and more efficient structures.

Acknowledgments

The author wishes to thank A. Levin and A. Sagi for the finite elements computations and R. Richards for proofing the paper.

References

[1] *ANSYS Users Manuals*, Swanson Analysis System, Inc., Houston, PA, May 1992.

[2] "PROBAN—The Probabilistic Analysis Program Manuals," DetNorske Veritas Research Repts., Hovik, Norway, June 1989.

[3] *Metallic Material and Elements for Aerospace Vehicles Structures*, MIL-HDBK-5F, Vol. 2, 1990.

[4] Montgomery, D. C., *Introduction to Linear Regression*, Wiley, New York, 1982, pp. 191, 192.

[5] Winterstein, S. R., "Nonlinear Responses and Fatigue Damage," *Journal of Engineering Mechanics*, Vol. 111, No. 10, 1985, pp. 1291–1295.

[6] Tvedt, L., "PROBAN Distribution Manual," DetNorske Veritas Research Rept. 89-2026, Hovik, Norway, 1989, pp. 22–24.

[7] Maymon, G., *Some Engineering Applications in Random Vibrations and Random Structures*, Vol. 178, Progress in Astronautics and Aeronautics, AIAA, Reston, VA, 1998, pp. 170–200.

I. E. Vas
Associate Editor